An Investigation of Chain Length Dependent Termination and Reaction Diffusion Controlled Termination during the Free Radical Photopolymerization of Multivinyl Monomers

Tara M. Lovestead,[†] Kathryn A. Berchtold,[†,‡] and Christopher N. Bowman*[,†,§]

Department of Chemical and Biological Engineering, University of Colorado, Boulder, Colorado 80309-0424; Materials Science & Technology Division, MST-7, Los Alamos National Laboratory, Mail Stop E-549, Los Alamos, New Mexico 87545; and Department of Restorative Dentistry, University of Colorado Health Sciences Center, Denver, Colorado 80045-0508

Received March 10, 2005; Revised Manuscript Received June 3, 2005

ABSTRACT: Recent investigations of dimethacrylate monomers reveal that chain length dependent termination (CLDT) is important during network formation; however, the importance is not a trivial function of double bond conversion or monomer chemistry. Poly(ethylene glycol)-600 dimethacrylate (PEG600DMA) simultaneously exhibits CLDT and reaction diffusion controlled termination and a reaction diffusion coefficient that depends on the cure condition. To investigate this behavior, the impact of light intensity, monomer chemistry, and network formation on the termination mechanism was investigated. The copolymerization of PEG600DMA with increasing di(ethylene glycol) dimethacrylate (DEGDMA) concentrations reveals that the importance of CLDT during reaction diffusion controlled termination is a function of the rubbery or glassy nature of the resulting polymer network. As well, the addition of nonreactive PEG600 to the DEGDMA polymerization increases the importance of CLDT throughout the polymerization and elevates the reaction diffusion coefficient. Finally, electron paramagnetic resonance (EPR) spectroscopy unsteady-state experiments reveal a strong chain length dependence of the termination kinetic constant for long radical chains during the high double bond conversion of both rubbery and glassy dimethacrylates.

Introduction

Dimethacrylate monomers photopolymerize to form highly cross-linked networks that afford increased strength, toughness, and chemical resistance as compared to linear polymers. The photopolymerization reaction occurs under ambient conditions, does not require a solvent, is rapid when compared to thermal polymerizations, and provides spatial and temporal control. For these numerous reasons photopolymer networks are attractive industrially and are used in a variety of applications, including dental materials, contact lenses, microelectronics, adhesives, coatings, and biomaterials.[1−5]

While industrially photopolymer networks are widely used, it is not well understood in many systems how changing the cure conditions (light intensity profile, initiator concentration, and temperature), monomer chemistries, and monomer functionalities affects the final polymer network and resulting material properties. This is, in part, due to the extremely complex termination kinetics that these monomers exhibit.[6−12] For example, recent investigations of dimethacrylate monomers reveal that chain length dependent termination (CLDT) is important during network formation. However, the importance of CLDT is not a trivial function of double bond conversion or monomer chemistry.[9,10] This paper aims to explore further termination during dimethacrylate network formation. An improved understanding of termination will lead to increased control of the photopolymerization process, the final polymer network structure, and the mechanical properties, thus increasing and improving applications.

The classical picture of the termination reaction is chain length independent, bimolecular termination, which is a three-step process. First, the center-of-mass of both radical chains must approach one another via translational or reaction diffusion. Then, the radical chain ends rearrange by segmental diffusion to place the radicals proximate enough for termination, which occurs through chemical reaction.[13−15] When classical, bimolecular, chain length independent termination and a pseudo-steady-state radical concentration are assumed, the polymerization rate (R_p) is expected to depend on the initiation rate (R_i) to the 1/2 power (eq 1).

$$R_p = \frac{k_p}{\sqrt{2k_t}}[C{=}C]R_i^{\alpha} \quad (1)$$

Here, k_p and k_t are the propagation and termination kinetic constants, respectively, [C=C] is the double bond concentration, and α is the scaling exponent that is 1/2 classically.[15−17]

Under typical photopolymerization conditions, multivinyl monomers have been shown to exhibit diffusion controlled kinetics throughout their polymerization. Diffusion control of the termination kinetic constant begins at the onset of the polymerization due to the almost instantaneous accumulation of high molecular weight and/or cross-linked polymer during polymerization and/or network formation. This decrease in the termination rate coupled with the double bond diffusion and propagation rates remaining rapid results in autoacceleration or the counterintuitive increase in the

[†] University of Colorado.
[‡] Los Alamos National Laboratory.
[§] University of Colorado Health Sciences Center.
* Corresponding author: e-mail Christopher.Bowman@colorado.edu; Fax 303 492 4341; Ph 303 492 3247.

10.1021/ma050519l CCC: $30.25
Published on Web 06/30/2005

polymerization rate with time.[17−21] Eventually, at greater double bond conversions, the double bond mobility is also hindered, and the propagation mechanism becomes diffusion controlled, resulting in autodeceleration or the rapid decrease in R_p with time. When the cure temperature is below the polymer's glass transition temperature (T_g), autodeceleration generates a limiting double bond conversion that is both monomer chemistry and functionality dependent.[22−24]

CLDT is also a result of diffusion limitations on the growing radical chain and dictates that the radical chain's ability to terminate depends on its molecular weight (kinetic chain length). Monomers that exhibit CLDT kinetics have an average termination kinetic constant that depends on the kinetic chain length distribution (KCLD) and any cure condition that impacts the KCLD.[14,24−27] For example, if increasing the initiation rate shifts the KCLD toward shorter average kinetic chain lengths and the termination mechanism is chain length dependent, then the more rapid short radical chain termination results in a less than classically expected increase in the polymerization rate. Thus, CLDT leads to a decrease in the overall scaling exponent, α (from eq 1). A less than classical scaling exponent α is observed often during monovinyl monomer polymerizations[14,24,28−32] and is attributed to CLDT kinetics. Recently, a less than classical α has also been shown to be important during dimethacrylate photopolymerization.[6,9−12,33,34]

Diffusion control of the termination mechanism during multivinyl monomer photopolymerization also results in reaction diffusion controlled termination. This termination regime becomes important when two radicals encounter each other more rapidly by "growing" toward each other through the addition of double bonds rather than by the radical simply moving through the space surrounding the chain end (segmental diffusion). Reaction diffusion controlled termination is characterized by the termination kinetic constant's dependence on the propagation frequency.[6,8,21,35−37] Analysis of the polymerization kinetics in the dark reveals the ratio of the kinetic constants ($k_t/(k_p[C{=}C])$) at the double bond conversion that the light is extinguished. When reaction diffusion controlled termination is the dominant termination mechanism, the ratio of the termination kinetic constant to the propagation frequency is constant, and a reaction diffusion coefficient (R, eq 2) defines the reacting system.

$$R = \frac{k_t}{k_p[C{=}C]} \tag{2}$$

Berchtold and co-workers have investigated the importance of CLDT and reaction diffusion controlled termination during the photopolymerization of di(ethylene glycol) dimethacrylate (DEGDMA).[6,9,10,33] They observed that DEGDMA exhibits α values less than 1/2, indicative of the importance of CLDT at low double bond conversions and a transition from CLDT to reaction diffusion controlled termination (a chain length independent mechanism) at high double bond conversions. Additionally, Anseth and co-workers[34] and Cook[11,12] have reported similar nonclassical behavior at low double bond conversions during network formation.

CLDT has been modeled extensively in diffusion controlled monovinyl (photo)polymerizations[20,25,27,29,31,38−53] and, thus, is generally accepted as important during monovinyl polymerization. Recently, a model of multivinyl monomer photopolymerization kinetics that takes into account CLDT was developed to investigate the impact of accounting for CLDT on the reaction kinetics.[33] The model builds upon prior models of multivinyl monomer photopolymerization.[22,54−56] The model predicts that CLDT is important primarily before and during autoacceleration when the mobility of short radical chains that are not tethered to the polymer network is dictated by their length. Additionally, the CLDT model predicts the aforementioned similar DEGDMA photopolymerization behavior experimentally observed by Berchtold and co-workers.[6]

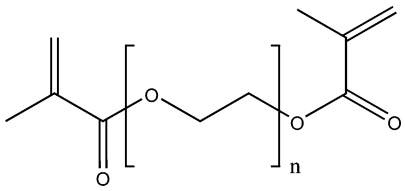

Figure 1. Chemical structures for DEGDMA (n = 2), TEGDMA (n = 3), and PEG600DMA (n = 14) are presented.

Recent investigations have revealed a more complex relationship between CLDT and reaction diffusion controlled termination. Berchtold and co-workers experimentally investigated the impact of the initiation rate on the polymerization rate of poly(ethylene glycol)-600 dimethacrylate (PEG600DMA).[6,9,10] They observed that PEG600DMA exhibits CLDT ($\alpha < 1/2$) throughout the entire polymerization. Additionally, PEG600DMA exhibits reaction diffusion controlled termination at moderate to high double bond conversions, i.e., $k_t/(k_p[C{=}C])$ plateaus. PEG600DMA is also unique from DEGDMA and other dimethacrylates in that its reaction diffusion coefficient (R, eq 2) increases when PEG600DMA is polymerized with higher initiation rates. Thus, PEG600DMA exhibits simultaneous CLDT ($\alpha < 1/2$) and reaction diffusion controlled termination ($k_t/(k_p[C{=}C])$ plateaus) and uniquely exhibits initiation rate dependent unsteady-state kinetics.

The aim of this work is to obtain a better understanding of CLDT kinetics throughout the polymerization by probing further the chain length dependent reaction diffusion controlled termination kinetics exhibited by PEG600DMA. First, the importance of the rubbery or glassy nature of the polymer network formed on the termination kinetics is examined by investigating the copolymerization of PEG600DMA with DEGDMA. These two monomers are interesting to study because they differ only in the number of ethylene glycol spacer units (Figure 1), which leads to the formation of either a rubbery (PEG600DMA) or glassy (DEGDMA) polymer network. Thus, the importance of either rubbery or glassy network formation on the termination kinetics is probed. Additionally, the impact of nonreactive PEG600 solvent addition to the DEGDMA polymerization is examined.

The termination mechanism is examined using Fourier transform infrared (FTIR) spectroscopy, which monitors the change in the double bond concentration with polymerization time. The impact of increasing the initiation rate on the polymerization rate ($R_p \propto R_i^{\alpha}$) is quantified as a function of double bond conversion by determining the scaling exponent, α, which reveals information about the complex termination mechanism throughout the polymerization. For example, an $\alpha < 1/2$ is indicative of CLDT and reveals that the termination

kinetics depends on the KCLD. Additionally, an $\alpha \sim 1/2$ is attributed to chain length independent, bimolecular termination kinetics. While not addressed specifically in this paper, an $\alpha > 1/2$ has also been attributed to the importance of unimolecular termination, i.e., persistent radical accumulation. FTIR spectroscopy is also utilized to examine the unsteady-state kinetics of both the PEG600DMA copolymerization with DEGDMA and the DEGDMA polymerization with the addition of nonreactive PEG600 solvent as a function of light intensity.

Finally, electron paramagnetic resonance (EPR) spectroscopy was used to monitor the radical concentration decay rate in the dark to obtain information about the chain length dependence of the termination kinetic constant for two monomers that form either a rubbery or glassy network. This is accomplished using an analytical technique recently developed by Buback and co-workers for the low double bond conversion of monovinyl methacrylates. While the analysis was developed for radical concentration decay profiles during the dark cure for systems that yield very monodisperse KCLDs, it is the only analytical technique for evaluating the chain length dependence of the termination kinetic constant. Additionally, while a homogeneous KCLD does not exist when the light is extinguished, a more homogeneous KCLD is approached at long times in the dark, and thus, the analytical technique is applied to multivinyl monomer photopolymerization kinetics for the first time. Thus, a series of experiments that probe the importance of CLDT and chain length dependent reaction diffusion controlled termination throughout multivinyl monomer photopolymerizations are presented. A more complete understanding of the complex termination mechanism will enable a more rational approach for designing and tuning monomer chemistry and cure conditions for specific end-use applications.

Experimental Section

Materials. This study utilized the following monomers: PEG600DMA (Figure 1, $n = 14$, Polysciences, Inc., Warrington, PA), DEGDMA (Figure 1, $n = 2$, Polysciences, Inc., Warrington, PA), and tri(ethylene glycol) dimethacrylate (TEGDMA, Figure 1, $n = 3$, Polysciences, Inc., Warrington, PA). Samples contain 0.1−1.0 wt % of the photoinitiator 2,2-dimethoxy-2-phenylacetophenone (DMPA, Ciba Geigy, Hawthorne, NY).

Irradiation Source. An ultraviolet (UV) light source (Acticure, 100 W Hg short-arc lamp, EXFO, Mississaugua, Ontario, Canada) equipped with a liquid light guide and a band-pass filter (320−390 nm, EXFO, Mississaugua, Ontario, Canada) was used to irradiate monomer mixtures. The incident light intensity is controlled via the internal aperture of the Acticure.

Methods. a. Fourier Transform Infrared (FTIR) Spectroscopy. A real-time FTIR spectrophotometer (Nicolet model 760 Magna Series II FTIR, Nicolet, Madison, WI) equipped with a MCT/B-XT KBr detector−beam splitter combination monitors the polymerization kinetics. A horizontal transmission accessory enables horizontal sample mounting for FTIR measurements.[57,58] Monomer/initiator mixtures for mid-FTIR analysis are sandwiched between NaCl crystals to obtain an approximately 10−30 μm thick sample. The mid-FTIR analyses scan the spectral range 600−3800 cm^{-1} and monitor double bond conversions by measuring the area of the C=C absorption (ca. 1637 cm^{-1}).[59]

FTIR spectroscopy is used to obtain information about the termination mechanism throughout the polymerization, i.e., to determine α for the photopolymerization, where α describes the relationship between the polymerization rate and the initiation rate ($R_p \propto R_i^{\alpha}$). First, the change in the methacrylate double bond peak is monitored as a function of polymerization time. Then, the derivative of the FTIR data is taken to provide the polymerization rate as a function of time, which is directly correlated to R_p as a function of double bond conversion. Data are collected for at least two initiation rates. Least-squares analysis is then used to fit an α so that the sum of the squared error between R_p/R_i^{α} for each initiation condition at a given double bond conversion is minimized (i.e., the error is less than 10^{-6}). α values were calculated for photopolymerizations at 0.5 and 20 mW/cm^2 with 1 wt % DMPA.

The α analysis was developed to account for exponential decay of the initiator concentration ([*Ab*], eq 3) with polymerization time and assumes that the molar absorptivity (ϵ) for DMPA at the peak initiating wavelength ($\lambda = 365$ nm) is 150 L/(mol cm). Equation 4 then describes the change in the initiation rate with polymerization time.

$$\frac{d[Ab]}{dt} = \frac{-2.303\epsilon[Ab]I_{inc}\lambda}{N_{Av}hc} \tag{3}$$

$$R_i = 2\phi I_a = 2\phi\left(\frac{2.303\epsilon[Ab]I_{inc}\lambda}{N_{Av}hc}\right) \tag{4}$$

Here, t is the polymerization time, I_{inc} is the incident light intensity in units of power/area, N_{Av} is Avogadro's number, h is Planck's constant, and c is the speed of light. Additionally, the 2 represents two radicals produced per initiator molecule photocleaving,[60] ϕ is the fraction of absorbed photons that initiate polymerization and is assumed to be unity, and I_a is the photon absorption rate.[61] It is important to note that the scaling of the polymerization behavior with initiation rate is of primary importance in these studies, not the absolute value of the initiation rate. The assumptions of unity for the efficiency and 2 radicals produced per initiator molecule photocleaving will, thus, have minimal impact on the scaling.

FTIR spectroscopy was also used to examine the polymerization kinetics during the dark reaction (i.e., the unsteady-state kinetics). In the absence of initiation, the change in the radical concentration is due only to radical termination. The unsteady-state analysis takes into account bimolecular, chain length independent termination according to eq 5:

$$\frac{d[P^{\bullet}]}{dt_{dark}} = -2k_t[P^{\bullet}]^2 \tag{5}$$

where [P•] is the radical concentration. Upon integration, eq 5 provides an expression for the radical concentration as a function of time. This expression is then substituted in the expression for the change in the double bond concentration with dark polymerization time (eq 6), which upon rearrangement provides eq 7.

$$\frac{d[C{=}C]}{dt_{dark}} = -k_p[C{=}C][P^{\bullet}] \tag{6}$$

$$\Delta[C{=}C] = \frac{1}{2R}\ln(2RR_{p0}t_{dark} + 1) \tag{7}$$

The change in the double bond concentration (Δ[C=C]) with dark polymerization time (t_{dark}) depends only on the polymerization rate at time zero in the dark (R_{p0}) and the ratio of the termination kinetic constant to the propagation frequency (R from eq 2). The R value that provides the best fit of eq 7 to the FTIR unsteady-state data describes the ratio of the termination kinetic constant to the propagation frequency at the double bond conversion that the light was extinguished. R values are obtained at several different double bond conversions, and the double bond conversion at which R plateaus is indicative of the termination mechanism occurring predominantly via reaction diffusion controlled termination. A more complete description of the unsteady-state kinetic analysis is provided by Anseth and co-workers.[3]

b. Dynamic Mechanical Analysis (DMA). A dynamic mechanical analyzer (DMA7e, Perkin-Elmer, Norwalk, CT) was used to obtain the glass transition temperature (T_g) region for the resulting polymer networks using extension mode. Samples were polymerized at room temperature using 320−390 nm UV light at 5 mW/cm^2 with 1 wt % DMPA in the geometry necessary for DMA ($7 \times 3 \times 1$ mm^3). The loss tangent was recorded over a temperature range of −50 to 300 °C. The temperature was increased at a rate of 5 °C/min. The T_g was taken as the temperature that the loss tangent curve achieved its maximum value. Analyses were performed in triplicate.

c. Electron Paramagnetic Resonance (EPR) Spectroscopy. An EPR spectrophotometer (ESP300E Bruker Analytik GmbH, Rheinstetten/Karlsruhe, Germany) operating in the X-band was used to monitor the radical concentrations throughout the polymerization. A TE_{102} cavity, operating at a 100 kHz field modulation frequency and at a 2 G_{pp} field modulation amplitude, was used.

All monomer/initiator mixtures are purged with nitrogen gas for 10 min. 1 mm i.d. capillary tubes are filled with equal sample volumes and flame-sealed under a nitrogen purge. The capillary tubes are placed in a thick-walled quartz EPR sample tube (Wilmad precision quartz model 700-PQ-7 sample tube, 1.40 mm wall thickness, 2.16 mm i.d., Wilmad Glass, Buena, NJ) and then into a TE_{102} cavity for analysis. A double-walled quartz dewar insert (Wilmad Suprasil Quartz dewar insert, model 821-F-Q, Wilmad Glass, Buena, NJ) is inserted in the cavity, which allows for cavity temperature control and increased cavity sensitivity. The microwave cavity was purged with nitrogen gas to eliminate the background oxygen signal.

Sample irradiation and EPR spectroscopic measurement are concurrent; thus, the EPR monitors the radical concentration profile during photopolymerization. The α,α′-diphenyl-1-picrylhydrazyl (DPPH, Aldrich, Milwaukee, WI) calibration curve correlates the EPR spectra's intensity to radical concentration. All experiments are at 25 °C. A more detailed discussion of EPR spectroscopy parameter selection, DPPH concentration calibration, polymerization characterization, and EPR analysis is in ref 62.

Results and Discussion

FTIR Spectroscopy. PEG600DMA and DEGDMA are similar in chemistry and functionality but form rubbery and glassy polymer networks, respectively. To examine the hypothesis that the nature of the polymer network formed impacts the importance of CLDT throughout the polymerization and to investigate the impact of network formation on the initiation rate dependence of PEG600DMA's reaction diffusion coefficient, DEGDMA was copolymerized with increasing PEG600DMA concentration.

Dynamic mechanical analysis (DMA) reveals that increasing the PEG600DMA composition results in a decrease in the glass transition temperature of the resulting copolymer network ($T_g \sim 110$, 35, 10, and −30 °C for 0, 65, 80, and 100 wt % PEG600DMA, respectively). Additionally, increasing the PEG600DMA concentration of the comonomer mixture increases the final double bond conversion achieved and decreases the breadth of the resulting polymer network's glass transition temperature region.

The impact of the rubbery or glassy polymer formation on CLDT and chain length dependent reaction diffusion controlled termination was investigated utilizing FTIR spectroscopy to evaluate the dependence of the polymerization rate on the initiation rate. Figure 2 reveals that copolymerizing DEGDMA with 65 wt % PEG600DMA increases the importance of CLDT beyond 20% double bond conversion and a transition from CLDT important kinetics ($\alpha < 1/2$) to a chain length independent termination mechanism ($\alpha \sim 1/2$) is observed at ∼65% double bond conversion. The DEGDMA copolymerization with 80 wt % PEG600DMA exhibits CLDT kinetics ($\alpha < 1/2$) throughout the entire polymerization. Thus, these results suggest that the importance of CLDT at high double bond conversion depends on the rubbery or glassy nature of the resulting polymer network. Additionally, several termination mechanisms may be important during network formation, especially when the polymerization occurs below the resulting network's T_g. For example, if termination occurs by both unimolecular termination and chain length dependent bimolecular termination, mechanisms characterized by a scaling exponent of $\alpha > 1/2$ and $\alpha < 1/2$, respectively, the system may exhibit an average scaling exponent of $\alpha \sim 1/2$.

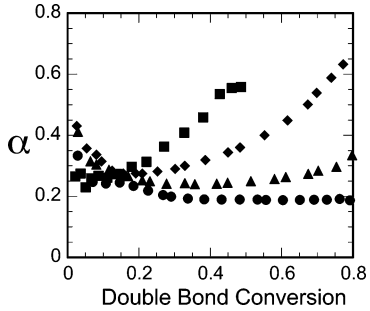

Figure 2. α is presented as a function of double bond conversion for the copolymerization of DEGDMA with PEG600-DMA (0 (■), 65 (◆), 80 (▲), and 100 wt % (●) PEG600DMA).

The impact of the resulting copolymer's T_g region on the termination kinetics was investigated further by examining the impact of curing temperature on the importance of CLDT throughout the polymerization. Increasing the cure temperature from 25 to 70 °C did not impact the CLDT behaviors that bulk PEG600DMA and DEGDMA exhibit. While this behavior was anticipated for the homopolymerization, both of the copolymer networks exhibit very broad glass transition temperature regions that overlap with the ambient cure temperature, and thus, the impact of the cure temperature on these systems was also investigated. Interestingly, the DEGDMA copolymerization with either 65 or 80 wt % PEG600DMA is affected minimally by increasing the cure temperature (Figure 3), especially at greater double bond conversions where the increased mobility due to increased curing temperature would have the greatest impact on the reaction kinetics.

To investigate further the importance of CLDT at high double bond conversions during the copolymerization of DEGDMA with PEG600DMA, the unsteady-state kinetics were examined as a function of light intensity. Table 1 presents the reaction diffusion coefficient (R) in the plateau region for bulk PEG600DMA and DEGDMA polymerizations and the copolymerization of DEGDMA with 80 wt % PEG600DMA. The steady-state copolymerization kinetics for this system exhibit CLDT throughout the entire polymerization (Figure 3); however, the unsteady-state copolymerization kinetics exhibit a plateau in the ratio of the termination kinetic constant to the propagation frequency (the R value) that is nearly independent of the initiation rate. Thus, the copolymerization of DEGDMA with 80 wt % PEG600-DMA exhibits steady-state polymerization kinetics indicative of the importance of CLDT at very high double bond conversions; however, the unsteady-state polymerization kinetics reveal an R value that depends weakly on the initiation rate (Table 1).

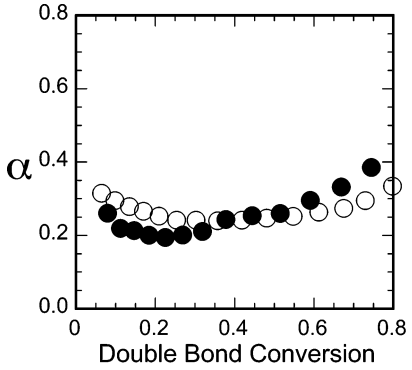

(a)

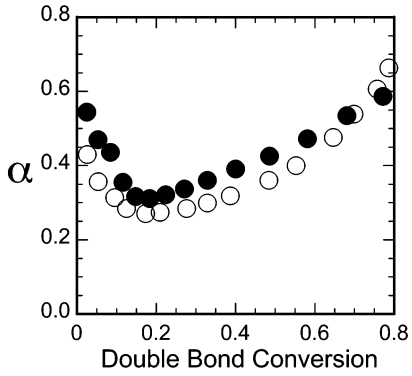

(b)

Figure 3. α is presented as a function of double bond conversion for the copolymerization of DEGDMA with 80 (a) and 65 wt % (b) PEG600DMA. α is presented for polymerizations at 25 (○) and 70 °C (●).

Table 1. Reaction Diffusion Coefficients as a Function of Monomer Chemistry and Light Intensity[a]

monomer system	R (0.5 mW/cm^2)	R (20 mW/cm^2)
DEGDMA	2.7 ± 0.5	2.8 ± 0.4
PEG600DMA	2.7 ± 0.6	8.0 ± 1.0
20/80 wt % DEGDMA/PEG600DMA	2.4 ± 0.4	2.9 ± 0.1

[a] All polymerizations are initiated with 1 wt % DMPA.

The different CLDT behaviors exhibited by DEGDMA and PEG600DMA were investigated further. Specifically, the impact of the addition of nonreactive PEG600 solvent to the DEGDMA polymerization was investigated. Figure 4 reveals that increasing the PEG600 solvent concentration increases the polymerization rate at the onset of the polymerization, shifts the maximum polymerization rate to lower double bond conversions, and decreases the autodeceleration rate, which enables 100% conversion of the methacrylate double bonds. Furthermore, the addition of PEG600 solvent increases the importance of CLDT (i.e., $\alpha < 1/2$) for the majority of the DEGDMA photopolymerization (Figure 5).

The unsteady-state kinetics exhibited by the DEGDMA polymerization with the addition of nonreactive PEG600 is also examined. Polymerizing DEGDMA with the addition of 70 wt % of nonreactive PEG600 results in an elevated reaction diffusion coefficient; however, the elevation in the R value is independent of the light intensity ($R \sim 5.7 \pm 1.3$ and 6.0 ± 1.6 when irradiated at 0.5 and 20 mW/cm^2, respectively). These results suggest that polymerizing DEGDMA in the presence of nonreactive PEG600 increases the importance of CLDT throughout the polymerization and

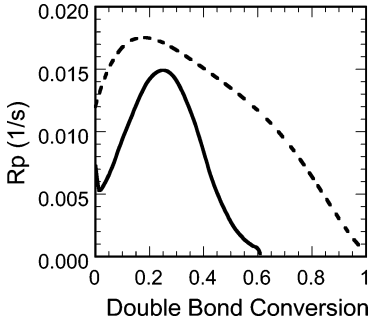

Figure 4. Polymerization rate as a function of double bond conversion for bulk DEGDMA (—) and DEGDMA with the addition of 70 wt % nonreactive PEG600 (- - -). All polymerizations are at 0.5 mW/cm^2 with 1 wt % DMPA.

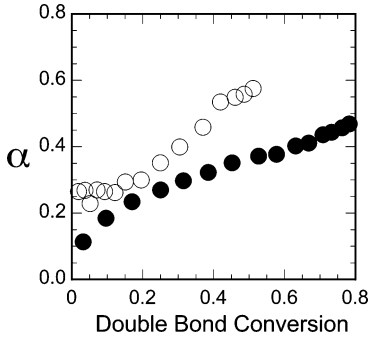

Figure 5. α is presented as a function of double bond conversion for bulk DEGDMA (○) and DEGDMA with the addition of 70 wt % nonreactive PEG600 (●).

elevates the termination kinetics during reaction diffusion controlled termination; however, a chain length independent reaction diffusion coefficient is observed. Additionally, these results suggest that the unique CLDT kinetics exhibited by PEG600DMA are possibly due to enhanced radical termination in the presence of PEG600DMA monomer or very short poly(PEG600DMA) kinetic chains.

EPR Spectroscopy. The analysis of the unsteady-state kinetics obtained via FTIR spectroscopy assumes chain length independent bimolecular termination. Recently, Buback and co-workers developed an analytical method to determine the chain length dependence of the termination kinetic constant for monomethacrylate monomers.[63] They utilized the experimental procedure of SP-PLP-EPR (single-pulse pulsed-laser-polymerization EPR). In this experiment a single laser pulse rapidly generates the radicals that initiate kinetic chains. The instantaneous generation of reactive radicals results in radical chains that grow nearly uniformly in the dark according to eq 8.

$$i \approx k_p[\mathrm{C{=}C}]t \tag{8}$$

Here, i is the degree of polymerization, k_p is the propagation kinetic constant, [C=C] is the double bond concentration, and t is the dark time. EPR spectroscopy is then used to monitor the bimolecular termination kinetic constant between two radical chains of equal chain length (eq 9).

$$-\frac{\mathrm{d}[\mathrm{P}^\bullet]}{\mathrm{d}t} = 2k_t^{i,i}[\mathrm{P}^\bullet]^2 \tag{9}$$

Here, [P•] is the radical concentration and $k_t^{i,i}$ is the termination kinetic constant of two radical chains of

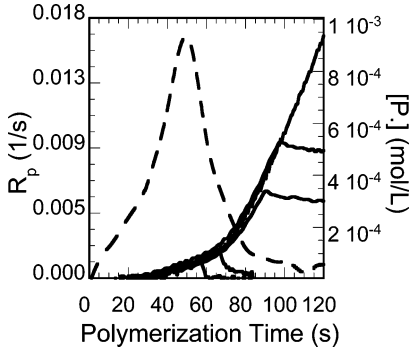

Figure 6. Polymerization rate (- - -) as a function of polymerization time for TEGDMA at 5 mW/cm^2 with 0.1 wt % DMPA is presented. Additionally, the radical concentration (—) for different polymerization times that the light is extinguished is presented. Radical concentrations are monitored via EPR spectroscopy.

equal chain length, i. However, since the degree of polymerization increases with increasing dark time, the dependence of $k_t^{i,i}$ on radical chain length is taken into account using a power-law relationship for the chain length dependence of k_t ($k_t^{i,i} = k_{t0}i^{-\varphi}$, where φ is the extent of chain length dependence), resulting in eq 10.

$$-\frac{d[P^\bullet]}{dt} = 2k_{t0}i^{-\varphi}[P^\bullet]^2 \qquad (10)$$

The rearrangement of the integrated form of eq 10 following substitution of the expression for the degree of polymerization results in eq 11.

$$\frac{[P^\bullet]_0}{[P^\bullet]_t} - 1 = \frac{2k_{t0}[P^\bullet]_0}{(1-\varphi)(k_p[C{=}C])^\varphi}t^{1-\varphi} \qquad (11)$$

Here, $[P^\bullet]_0$ is the radical concentration when the light is extinguished (time zero in the dark) and $[P^\bullet]_t$ is the radical concentration at time t in the dark. The slope of a double-log plot of eq 11 provides information about the chain length dependence of the termination kinetic constant, i.e., the slope is equal to $1 - \varphi$.

In this work EPR spectroscopy monitors the radical concentrations of PEG600DMA and tri(ethylene glycol) dimethacrylate (TEGDMA). TEGDMA is a monomer that differs from DEGDMA by only one ethylene glycol spacer unit and exhibits termination kinetics similar to DEGDMA, i.e., a transition from an α value less than classical to a value greater than classical at greater double bond conversions. EPR spectroscopy is used to ascertain the impact of rubbery and glassy network formation on the polymerization kinetics that these monomers exhibit during the dark reaction. Figure 6 presents the radical concentration profiles for several unsteady-state experiments; i.e., the monomers are irradiated for various polymerization times prior to extinguishing the light. The polymerization rate as a function of polymerization time for continuous irradiation is also presented.

One difference between the unsteady-state method presented here and the SP-PLP-EPR method developed by Buback and co-workers is that the SP-PLP-EPR method generates a homogeneous radical chain length distribution. In this unsteady-state technique, a heterogeneous radical chain length distribution exists when the light is extinguished during the multivinyl monomer unsteady-state experiment. Thus, the analysis for determining the chain length dependence of the termination kinetic constant clearly does not apply to the network formation unsteady-state experiment at short dark polymerization times. However, in the absence of chain transfer, the distribution of radical chains that survive termination all grow to approximately equivalent degrees of polymerization (i, eq 8) at long times in the dark when i during the dark polymerization is much greater than the radical length at the time the light is extinguished. Hence, a more homogeneous distribution of radical chains is approached at long times in the dark. Thus, EPR spectroscopy and Buback and co-worker's analysis provide information about that chain length dependence of the termination kinetic constant for long chains during the dark polymerization of network forming monomers.

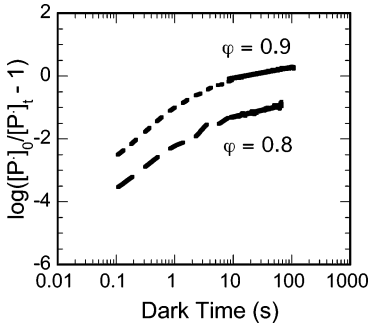

Figure 7. A double-log plot from the radical concentration decay data obtained via EPR spectroscopy according to eq 11 for 90 s of TEGDMA (- - -) and 50 s of PEG600DMA (• • •) irradiation (~60 and 90% double bond conversion, respectively). The straight lines are the best linear fits to the long (10−100 s) dark times. The slope of the linear fits, $1 - \varphi$, reveals the extent of k_t's chain length dependence. All polymerizations are at 5 mW/cm^2 with 0.1 wt % DMPA.

Figure 7 presents a double-log plot of eq 11 for the radical concentration data obtained during the dark polymerization of TEGDMA and PEG600DMA (light off at 60 and 90% double bond conversion, respectively). A representative data set for each monomer when the light was extinguished after at least 30% double bond conversion is presented. Prior to 30% double bond conversion, the radical concentration decays too rapidly to obtain data beyond 2 s of dark time. The slopes of the best linear fit to the EPR data reveal a very strong dependence of the termination kinetic constant on the radical chain length at long dark polymerization times.

To test the validity of this approach, a simulated EPR experiment was performed using the model of Lovestead and co-workers.[6,33] This simulated dark experiment was then analyzed by the same method of Buback and co-workers.[63] The model is a useful tool for analyzing the polymerization kinetics of multivinyl monomers during network formation because it accounts for radical chains of each length and thus predicts the impact of CLDT on the polymerization kinetics. Additionally, the model predicts polymerization behaviors typically observed during network formation, i.e., autoacceleration, reaction diffusion controlled termination, and incomplete double bond conversion. The model that utilizes the material properties for DEGDMA and the model parameters for diffusion control and free volume effects on termination and propagation appears in Lovestead et al.[64] The scaling exponent ($\varphi = 0.8$) was selected to describe the experimentally observed CLDT behavior that DEGDMA exhibits when polymerized with 1.0 wt % DMPA at both 0.5 and 20 mW/cm^2. Interestingly, the

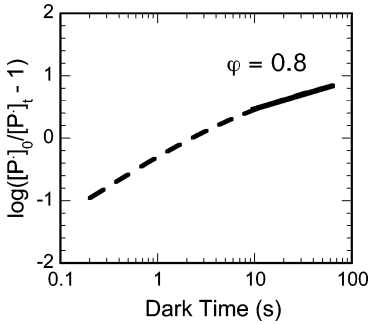

Figure 8. A double-log plot from the radical concentration decay as predicted by a CLDT model simulation according to eq 11 of DEGDMA polymerization where R_i is 0 at 50% double bond conversion. The straight line is the best linear fit to the long (10−100 s) dark times. The slope of the linear fits, $1 - \varphi$, reveals the extent of k_t's chain length dependence. The polymerization is simulated at 5 mW/cm^2 with 0.1 wt % DMPA.

model reveals that a φ of 0.8 is predicted after 10 s of dark polymerization time (Figure 8). Thus, the model reveals that the analysis does not provide accurately the extent of chain length dependence of the termination kinetic constant during network formation at low dark times but may do so for longer times.

The experimental results for TEGDMA and PEG600-DMA reveal strong chain length dependence of the termination kinetic constant ($\varphi = 0.8$) for long chains during the dark polymerization of network forming monomers. Buback et al. report a different phenomenon. They investigated the chain length dependence of the termination kinetic constant for a dodecyl methacrylate and observed that chain length dependencies decrease with increasing dark polymerization time (i.e., φ is ∼0.5 and ∼0.2 for short and long times, respectively, in the dark). The change in the dependence of k_t on the radical chain length is attributed to the termination mechanism transitioning from translational to segmental diffusion control. On the basis of the results that Buback and coworkers report, it was expected that the EPR spectroscopy experiment would reveal a weak dependence of the dark termination kinetics on radical chain length during multivinyl monomer photopolymerizations, especially at high double bond conversions when termination is thought to occur predominantly via reaction diffusion controlled termination. While the observed strong chain length dependence of the termination kinetic constant is not fully understood, it is an interesting result.

Conclusions

The origin of the different CLDT kinetics exhibited by glassy and rubbery network forming dimethacrylates was investigated to elucidate the nature of PEG600-DMA's simultaneous exhibition of chain length dependent and reaction diffusion controlled termination. The copolymerization of DEGDMA with the addition of PEG600DMA reveals that decreasing the T_g region of the resulting copolymer network increases the importance of CLDT throughout the polymerization; however, R is not initiation rate dependent. As well, the addition of nonreactive PEG600 solvent to the DEGDMA polymerization increases the importance of CLDT throughout the polymerization and elevates the reaction diffusion coefficient; however, a chain length independent R value is observed in contrast to the PEG600DMA polymerization. Finally, unsteady-state EPR experiments reveal a strong chain length dependence of the termination kinetic constant for long radical chains during the high double bond conversion of both rubbery and glassy dimethacrylates. Thus, a series of experiments are presented that probe the importance of CLDT and chain length dependent reaction diffusion controlled termination during network formation of both rubbery and glassy dimethacrylates.

Acknowledgment. The authors thank the I/UCRC for Fundamentals and Applications of Photopolymerizations and the United States Department of Education (DOE) for granting a GAANN fellowship to T.M.L. and K.A.B. Los Alamos National Laboratory is operated by the University of California for the United States DOE under Contract W-7405-ENG-36.

References and Notes

(1) Dickens, S. H.; Stansbury, J. W.; Choi, K. M.; Floyd, C. J. E. *Macromolecules* **2003**, *36*, 6043−6053.
(2) Anseth, K. S.; Metters, A. T.; Bryant, S. J.; Martens, P. J.; Elisseeff, J. H.; Bowman, C. N. *J. Controlled Release* **2002**, *78*, 199−209.
(3) Anseth, K. S.; Newman, S. M.; Bowman, C. N. *Adv. Polym. Sci.* **1995**, *122*, 177−217.
(4) Decker, C. *Acta Polym.* **1994**, *45*, 333−347.
(5) Kloosterboer, J. G. *Adv. Polym. Sci.* **1988**, *84*, 1−61.
(6) Berchtold, K. A.; Lovestead, T. M.; Bowman, C. N. *Macromolecules* **2002**, *35*, 7968−7975.
(7) Anseth, K. S.; Decker, C.; Bowman, C. N. *Macromolecules* **1995**, *28*, 4040−4043.
(8) Young, J. S.; Bowman, C. N. *Macromolecules* **1999**, *32*, 6073−6081.
(9) Berchtold, K. A.; Hacioglu, B.; Lovell, L.; Nie, J.; Bowman, C. N. *Macromolecules* **2001**, *34*, 5103−5111.
(10) Berchtold, K. A.; Lovell, L. G.; Nie, J.; Hacioglu, B.; Bowman, C. N. *Polymer* **2001**, *42*, 4925−4929.
(11) Cook, W. D. *J. Polym. Sci., Part A* **1993**, *31*, 1053−1067.
(12) Cook, W. D. *Polymer* **1992**, *33*, 600−609.
(13) Russell, G. T. *Macromol. Theory Simul.* **1995**, *4*, 497−517.
(14) Benson, S. W.; North, A. M. *J. Am. Chem. Soc.* **1962**, *84*, 935−940.
(15) North, A. M.; Reed, G. A. *J. Am. Chem. Soc.* **1961**, *83*, 9−870.
(16) Scherzer, T.; Decker, U. *Radiat. Phys. Chem.* **1999**, *55*, 615−619.
(17) Soh, S. K.; Sundberg, D. C. *J. Polym. Sci., Polym. Chem. Ed.* **1982**, *20*, 1299−1313.
(18) Korolev, G. V. *Russ. Chem. Rev.* **2003**, *72*, 197−216.
(19) Adams, M. E.; Russell, G. T.; Casey, B. S.; Gilbert, R. G.; Napper, D. H. *Macromolecules* **1990**, *23*, 4624−4634.
(20) Tulig, T. J.; Tirrell, M. *Macromolecules* **1981**, *14*, 1501−1511.
(21) Soh, S. K.; Sundberg, D. C. *J. Polym. Sci., Polym. Chem. Ed.* **1982**, *20*, 1315−1329.
(22) Marten, F. L.; Hamielec, A. E. *J. Appl. Polym. Sci.* **1982**, *27*, 489−505.
(23) Soh, S. K.; Sundberg, D. C. *J. Polym. Sci., Polym. Chem. Ed.* **1982**, *20*, 1331−1344.
(24) Allen, P. E. M.; Patrick, C. R. *Macromol. Chem.* **1961**, *47*, 154−167.
(25) Russell, G. T.; Gilbert, R. G.; Napper, D. H. *Macromolecules* **1992**, *25*, 2459−2469.
(26) Russell, G. T. *Macromol. Theory Simul.* **1995**, *4*, 519−548.
(27) Mahabadi, H. *Macromolecules* **1991**, *24*, 606−609.
(28) Buback, M.; Egorov, M.; Feldermann, A. *Macromolecules* **2004**, *37*, 1768−1776.
(29) Litvinenko, G. I.; Kaminsky, V. A. *Prog. React. Kinet.* **1994**, *19*, 139−193.
(30) Mahabadi, H. K.; O'Driscoll, K. F. *Macromolecules* **1977**, *10*, 55−58.
(31) Olaj, O. F.; Kornherr, A.; Vana, P.; Zoder, M.; Zifferer, G. *Macromol. Symp.* **2002**, *182*, 15−30.
(32) Soh, S. K.; Sundberg, D. C. *J. Polym. Sci., Polym. Chem. Ed.* **1982**, *20*, 1345−1371.
(33) Lovestead, T. M.; Berchtold, K. A.; Bowman, C. N. *Macromol. Theory Simul.* **2002**, *11*, 729−738.
(34) Anseth, K. S.; Kline, L. M.; Walker, T. A.; Anderson, K. J.; Bowman, C. N. *Macromolecules* **1995**, *28*, 2491−2499.

(35) Russell, G. T.; Napper, D. H.; Gilbert, R. G. *Macromolecules* **1988**, *21*, 2133−2140.
(36) Anseth, K. S.; Wang, C. M.; Bowman, C. N. *Macromolecules* **1994**, *27*, 650−655.
(37) Buback, M.; Huckestein, B.; Russell, G. T. *Macromol. Chem. Phys.* **1994**, *195*, 539−554.
(38) Olaj, O. F.; Kornherr, A.; Zifferer, G. *Macromol. Theory Simul.* **2001**, *10*, 881−890.
(39) Olaj, O. F.; Vana, P.; Kornherr, A.; Zifferer, G. *Macromol. Chem. Phys.* **1999**, *200*, 2031−2039.
(40) Olaj, O. F.; Kornherr, A.; Zifferer, G. *Macromol. Theory Simul.* **1998**, *7*, 501−508.
(41) O'Neil, G. A.; Torkelson, J. M. *Macromolecules* **1999**, *32*, 411−422.
(42) Buback, M.; Egorov, M.; Kaminsky, V. *Macromol. Theory Simul.* **1999**, *8*, 520−528.
(43) Nikitin, A. N.; Evseev, A. V. *Macromol. Theory Simul.* **1999**, *8*, 296−308.
(44) de Kock, J. B. L.; Klumperman, B.; van Herk, A. M.; German, A. L. *Macromolecules* **1997**, *30*, 6743−6753.
(45) Tobita, H. *Macromolecules* **1996**, *29*, 3073−3080.
(46) Scheren, P. A. G. M.; Russell, G. T.; Sangster, D. F.; Gilbert, R. G.; German, A. L. *Macromolecules* **1995**, *28*, 3637−3649.
(47) Russell, G. T. *Macromol. Theory Simul.* **1994**, *3*, 439−468.
(48) Russell, G. T.; Gilbert, R. G.; Napper, D. H. *Macromolecules* **1993**, *26*, 3538−3552.
(49) Bamford, C. H. *Eur. Polym. J.* **1989**, *25*, 683−689.
(50) Zhu, S.; Hamielec, A. E. *Macromolecules* **1989**, *22*, 3093−3098.
(51) Olaj, O. F.; Zifferer, G.; Gleixner, G. *Macromolecules* **1987**, *20*, 839−850.
(52) Olaj, O. F.; Zifferer, G. *Macromolecules* **1987**, *20*, 850−861.
(53) Mahabadi, H. *Macromolecules* **1985**, *18*, 1319−1324.
(54) Goodner, M. D.; Bowman, C. N. *Chem. Eng. Sci.* **2002**, *57*, 887−900.
(55) Bowman, C. N.; Peppas, N. A. *Macromolecules* **1991**, *24*, 1914−1920.
(56) Anseth, K. S.; Bowman, C. N. *Polym. React. Eng.* **1992**−**93**, *1*, 4999−4520.
(57) Berchtold, K. A.; Bowman, C. N. In *RadTech Europe 99 Conference Proceedings, Berlin, Germany, November*, 1999; p 767.
(58) Lovell, L. G.; Berchtold, K. A.; Elliott, J. E.; Lu, H.; Bowman, C. N. *Polym. Adv. Technol.* **2001**, *12*, 335−345.
(59) Berchtold, K. In Department of Chemical Engineering, University of Colorado, Boulder, 2001.
(60) Groenenboom, C. J.; Hageman, H. J.; Overeem, T.; Weber, A. J. M. *Macromol. Chem.* **1982**, *183*, 281−292.
(61) Odian, G. *Principles of Polymerization*, 3rd ed.; John Wiley & Sons: New York, 1991.
(62) Berchtold, K. A.; Randolph, T. W.; Bowman, C. N. *Macromolecules,* submitted for publication.
(63) Buback, M.; Egorov, M.; Junkers, T.; Panchenko, E. *Macromol. Rapid Commun.* **2004**, *25*, 1004−1009.
(64) Lovestead, T. M.; Burdick, J. A.; Anseth, K. S.; Bowman, C. N. *Polymer*, in press.

MA050519L